Coupled Systems Mechanics, *Vol. 9, No. 6 (2020) 499-519*
DOI: https://doi.org/10.12989/csm.2020.9.6.499

Thermo-mechanical behavior of porous FG plate resting on the Winkler-Pasternak foundation

Benferhat Rabia[1,2], Hassaine Daouadji Tahar*[1,2] and Rabahi Abderezak[1,2]

[1]*Département de Génie Civil, Université Ibn Khaldoun Tiaret; BP 78 Zaaroura, Tiaret, Algérie*
[2]*Laboratoire de Géomatique et Développement Durable, Université de Tiaret, Algérie*

(Received November 16, 2019, Revised September 28, 2020, Accepted September 30, 2020)

Abstract. The effect of porosity on the thermo-mechanical behavior of simply supported functionally graded plate reposed on the Winkler-Pasternak foundation is investigated analytically in the present paper using new refined hyperbolic shear deformation plate theory. Both even and uneven distribution of porosity are taken into account and the effective properties of FG plates with porosity are defined by theoretical formula with an additional term of porosity. The present formulation is based on a refined higher order shear deformation theory, which is based on four variables and it still accounts for parabolic distribution of the transverse shearing strains and stresses through the thickness of the FG plate and takes into account the various distribution shape of porosity. The elastic foundation is described by the Winkler-Pasternak model. A new modified power-law formulation is used to describe the material properties of FGM plates in the thickness direction. The closed form solutions are obtained by using Navier technique. The present results are verified in comparison with the published ones in the literature. The results show that the dimensionless and stresses are affected by the porosity volume fraction, constituent volume fraction, and thermal load.

Keywords: FGM plate; porosity; thermo-mechanical behavior; Winkler-Pasternak foundations

1. Introduction

Currently, functionally graded materials (FGMs) are alternative materials commonly used in many kinds of engineering structures: aerospace, nuclear, civil, automotive, biomechanical, electronic, chemical, and mechanical industries. In fact, FGMs have been developed and successfully used in industrial applications since 1980's (Koizumi 1993). The most well-known FGM is compositionally graded from a ceramic to metal to incorporate such diverse properties as heat, wear, and oxidation resistance of ceramics with the toughness, strength, machinability, and bending capability of metals.

The plates under different mechanical applications may be subjected to different loads. Therefore, the knowledge of the characteristics of FGM plates is of much practical importance for the design of plates. From the literature, it should be noted that the behavior of plates resting on the Winkler-Pasternak foundation subjected to a thermo-mechanical loading drew the intention of many researchers (Adim 2016b, Benferhat 2018, Rabia 2016a, Hassaine Daouadji 2012a). The plates supported by an elastic foundation are very common in structural engineering. To describe the

*Corresponding author, Professor, E-mail: daouadjitahar@gmail.com

http://www.techno-press.org/?journal=csm&subpage=8 ISSN: 2234-2184 (Print), 2234-2192 (Online)

interaction between the plate and foundation, several foundation models have been proposed. The simplest one is the Winkler or one-parameter model (Winkler 1867). In this model, it is assumed that there is a proportional interaction between pressure and deflection of the applied point in the foundation. This model was improved by Pasternak (1954) by adding a shear spring to simulate the interactions between the separated springs in the Winkler model. The Pasternak or two-parameter model is widely used to describe the mechanical behavior of structure foundation interactions and will be used here to simulate the interactions between the plate and foundation (Belkacem 2016b, Benferhat 2019a, Hassaine Daouadji 2016c, Hadji 2015, Mohamed Amine 2019 and Bekki 2019).

Many studies have been conducted on the mechanical and thermo-mechanical behavior of FGM structures. Zenkour (2010) performed A hygrothermal bending analysis is presented for a functionally graded material (FGM) plate resting on elastic foundations. The elastic coefficients, thermal coefficient and moisture expansion coefficient of the plate are assumed to be graded in the thickness direction. Tinh (2016) presented the new numerical results of high temperature mechanical behaviors of heated FG plates, emphasizing the high temperature effects on static and dynamic response. Yaghoobi (2014) studied the nonlinear vibration and post-buckling analysis of beams made of functionally graded materials (FGMs) resting on nonlinear elastic foundation subjected to thermo-mechanical loading. Shuohui (2016) developed a novel and effective approach based on isogeometric analysis (IGA) and higher-order shear deformation theory (HSDT) for the Numerical results of buckling and free vibration of functionally graded plates considering in-plane material inhomogeneity. Bouderba (2013) presented an analytical solution to the thermo-mechanical bending response of FG plates resting on Winkler-Pasternak elastic foundations using a refined trigonometric shear deformation theory (RTSDT). Pakar (2018) studied the nonlinear vibrations of the unsymmetrical laminated composite beam (LCB) on a nonlinear elastic foundation where the governing equation of the problem is derived by using Galerkin method. Thom (2017) proposed a new third-order shear deformation plate theory (TSDT) for numerical analysis of buckling and bending behaviors of 2D-FGM plates without the need for special treatment of shear-locking effect and shear correction factors. Thanh Banh (2018) contributes to evaluate multiphase topology optimization design of plate-like structures on elastic foundations by using classic plate theory. Multi-material optimal topology and shape are produced as an alternative to provide reasonable material assignments based on stress distributions. Reddy (2001) investigated thermo-mechanical deformations of simply supported, functionally graded rectangular plates by using an asymptotic method (Belkacem 2016a, Benferhat 2019b, Hassaine Daouadji 2013). The temperature, displacements and stresses of the plate are computed for different volume fractions of the ceramic and metallic constituents. Bouderba (2018) analyzed bending analysis of FGM rectangular plates resting on non- uniform elastic foundations in thermal environment. Tan-Van (2018) integrated a novel numerical method based on the Moving Kriging (MK) interpolation meshfree method with a simple higher-order shear deformation plate theory to studied the static bending, free vibration and buckling of functionally graded (FG) plates. Isavand (2015) investigated the dynamic response of functionally gradient steel (FGS) composite cylindrical panels in steady-state thermal environments subjected to impulsive loads. Yadwinder (2018) developed non-polynomial shear deformation theories are assessed for thermo-mechanical response characteristics of laminated composite plates. Esfahani (2013) examined a thermal buckling and post-buckling analysis of functionally graded material (FGM) Timoshenko beams resting on a non-linear elastic foundation. Thermal and mechanical properties of the FGM media are considered to be functions of both temperature and position. Pandey (2017) presented a finite element formulation for thermal stress analysis of functionally graded material (FGM) sandwich beam subjected to thermal shock. A layerwise higher-

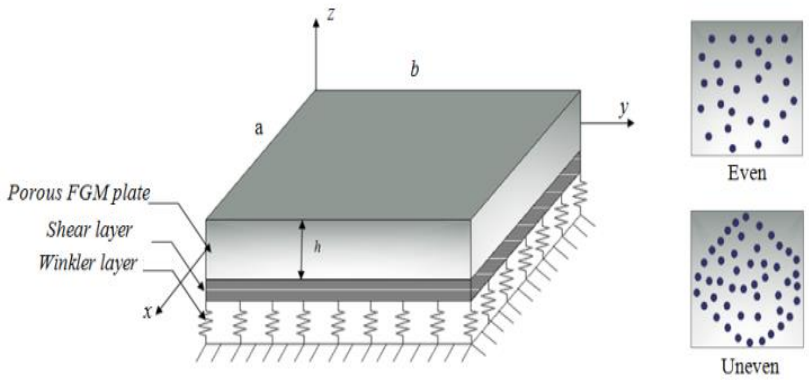

Fig. 1 Functionally graded porous plate resting on elastic foundation

order theory is used to obtain the stress-strain relationship for three layered functionally graded material sandwich beam. Babaei (2018) analyzed the nonlinear bending response of the functionally graded material curved tube subjected to the uniform lateral pressure. The effect of the thermal environment is also included (Abdelhak 2016, Adim 2016a, Rabia 2016b, Benhenni 2019, Hadji 2014, Benachour 2011, Tlidji 2014, Benferhat 2016b, Hassaine Daouadji 2017).

Recent investigations have been presented for the analysis of cracked FGM plates using advanced numerical methods. Liu (2015) developed an accurate extended 3-node triangular plate element in the context of the extended finite element method to study the buckling failure of cracked composite functionally graded plates subjected to uniaxial and biaxial compression loads. Shuohui (2015) extracted the critical buckling parameters and natural frequencies of defective FG plates with internal cracks using an effective numerical approach. Tiantang (2017) study the thermal-mechanical buckling of functionally graded rectangular and skew plates under combined thermal and mechanical loads.

Moreover, the effect of porosity on the behavior of FGMs has been the aim of just a few researchers. Benferhat (2016a) and Hassaine Daouadji (2016d), studied the static and free vibration analysis of FGM plates with porosities resting on elastic foundations. Heshmati (2018) presented the effect of different profile variations on vibrational properties of non-uniform beams made of graded porous materials. Wang (2018) studied the effect of porosities on free thermal vibration of functionally graded material (FGM) cylindrical shells by using the Loves shell theory to formulate the strain displacement equations, and the Rayleigh-Ritz method to calculate the natural frequencies of the system. To the authors' knowledge, no researchers have given much attention to thermo-mechanical loading of FGM plates containing porosities resting on elastic foundations. These porosities can occur within the FGM plates during the process of sintering. This is because of the large difference in solidification temperatures between material constituents (Zhu 2001).

This investigation aims to present the effect of the distribution shape of porosity on thermo-mechanical loading of FGM plates resting on Winkler-Pasternak foundations by using an improved version of hyperbolic shear deformation theory (Benferhat 2015, Hassaine Daouadji 2012b, Zohra 2016, Adim 2018, Benhenni 2018). Both even and uneven distribution shape of porosity are taken into account in this study by using a modified law of mixture. This theory is rather simple to use and accounts for a parabolic transverse shear deformation shape function and satisfies shear stress free boundary conditions of top and bottom surfaces of the plate without using shear correction factors.

Navier solution is used to obtain the closed-form solutions for simply supported functionally graded plates. Comparison studies are performed to verify the validity of the present results. The influences of several parameters are also discussed.

2. Theoretical formulation

The volumetric gradation of FGM plate containing porosities is shown in Fig. 1. In this figure, the top layer is made up of 100% ceramic and graded to 100% metal at the bottom. The porosities inside the shell disperse evenly or unevenly along the thickness direction. A simply supported square FGM plate with side length a in the x-direction, b in the y-direction and total thickness h is considered in this study.

For even and uneven types of effective properties are defined as (Benferhat 2016a, Rezaei 2017, Hassaine Daouadji 2016b and Pinar 2019)

Even distribution

$$\boldsymbol{P = (P_c - P_m)(\frac{1}{2} + \frac{z}{h})^k + P_m - (P_c + P_m)\frac{\beta}{2}} \tag{1}$$

Uneven distribution

$$\boldsymbol{P = (P_c - P_m)(\frac{1}{2} + \frac{z}{h})^k + P_m - \frac{\beta}{2}(P_c + P_m)(1 - \frac{2|z|}{h})} \tag{2}$$

where P is the effective material properties, k is the power law index and β is the porosity parameter. Subscript c and m denotes ceramic and metal, respectively.

Based on the higher order shear deformation plate theory, the displacement components are assumed to be:

$$\begin{gathered} u(x,y,z) = u_0(x,y) - z\frac{\partial w_b}{\partial x} - f(z)\frac{\partial w_s}{\partial x} \\ v(x,y,z) = v_0(x,y) - z\frac{\partial w_b}{\partial y} - f(z)\frac{\partial w_s}{\partial y} \\ w(x,y,z) = w_b(x,y) + w_s(x,y) \end{gathered} \tag{3}$$

where u_0 and v_0 are the in-plane displacements of the neutral plane in the x and y directions respectively. The transverse displacement through thickness direction is separated into bending (w_b) and shear (w_s) components. $f(z)$ is the shape function. In this paper hyperbolic shape function is used (Hassaine Daouadji 2016a)

$$f(z) = z\left[1 + \frac{3\pi}{2}sec\,\hbar^2(\frac{1}{2})\right] - \frac{3\pi}{2}\hbar\,tan\hbar(\frac{z}{\hbar}) \tag{4}$$

The origin of the material coordinates is at the middle surface of the plate. The linear strain can be obtained from kinematic relations as

$$\begin{gathered} \varepsilon_x = \varepsilon_x^0 + z\,k_x^b + (z\left[1 + \frac{3\pi}{2}sec\,\hbar^2(\frac{1}{2})\right] - \frac{3\pi}{2}\hbar\,tan\hbar(\frac{z}{\hbar}))\,k_x^s \\ \varepsilon_y = \varepsilon_y^0 + z\,k_y^b + (z\left[1 + \frac{3\pi}{2}sec\,\hbar^2(\frac{1}{2})\right] - \frac{3\pi}{2}\hbar\,tan\hbar(\frac{z}{\hbar}))\,k_y^s \\ \gamma_{xy} = \gamma_{xy}^0 + z\,k_{xy}^b + (z\left[1 + \frac{3\pi}{2}sec\,\hbar^2(\frac{1}{2})\right] - \frac{3\pi}{2}\hbar\,tan\hbar(\frac{z}{\hbar}))\,k_{xy}^s \\ \gamma_{yz} = g(z)\gamma_{yz}^s \end{gathered}$$

$$\gamma_{xz} = g(z)\gamma_{xz}^{s}$$
$$\varepsilon_z = 0 \tag{5}$$

Where

$$\varepsilon_x^0 = \frac{\partial u_0}{\partial x},\ k_x^b = -\frac{\partial^2 w_b}{\partial x^2},\ k_x^s = -\frac{\partial^2 w_s}{\partial x^2}$$
$$\varepsilon_y^0 = \frac{\partial v_0}{\partial y},\ k_y^b = -\frac{\partial^2 w_b}{\partial y^2},\ k_y^s = -\frac{\partial^2 w_s}{\partial y^2}$$
$$\gamma_{xy}^0 = \frac{\partial u_0}{\partial y} + \frac{\partial v_0}{\partial x},\ k_{xy}^b = -2\frac{\partial^2 w_b}{\partial x \partial y},\ k_{xy}^s = -2\frac{\partial^2 w_s}{\partial x \partial y}$$
$$\gamma_{yz}^s = \frac{\partial w_s}{\partial y},\ \gamma_{xz}^s = \frac{\partial w_s}{\partial x},$$
$$f'(z) = \frac{d\left(z\left[1 + \frac{3\pi}{2} sec\,\hbar^2\left(\frac{1}{2}\right)\right] - \frac{3\pi}{2}\hbar\, tan\hbar\left(\frac{z}{\hbar}\right)\right)}{dz}$$
$$g(z) = 1 - f'(z) = 1 - \frac{d\left(z\left[1+\frac{3\pi}{2} sec\,\hbar^2\left(\frac{1}{2}\right)\right] - \frac{3\pi}{2}\hbar\, tan\hbar\left(\frac{z}{\hbar}\right)\right)}{dz}, \tag{6}$$

Constitutive relations for linear elastic functionally graded plate can be given:

$$\begin{Bmatrix} \sigma_x \\ \sigma_y \\ \tau_{yz} \\ \tau_{xz} \\ \tau_{xy} \end{Bmatrix} = \begin{bmatrix} \frac{E(z)}{1-\nu^2} & \frac{\nu E(z)}{1-\nu^2} & 0 & 0 & 0 \\ \frac{\nu E(z)}{1-\nu^2} & \frac{E(z)}{1-\nu^2} & 0 & 0 & 0 \\ 0 & 0 & \frac{E(z)}{2(1+\nu)} & 0 & 0 \\ 0 & 0 & 0 & \frac{E(z)}{2(1+\nu)} & 0 \\ 0 & 0 & 0 & 0 & \frac{E(z)}{2(1+\nu)} \end{bmatrix} \begin{Bmatrix} \varepsilon_x - \alpha\Delta T \\ \varepsilon_y - \alpha\Delta T \\ \gamma_{yz} \\ \gamma_{xz} \\ \gamma_{xy} \end{Bmatrix} \tag{7}$$

where $\Delta T = T - T_0$ is the temperature rise from the reference temperature T_0.
where the temperature distribution *T(x, y, z)* through the thickness is assumed to be

$$T(x, y, z) = T_1(x, y) + \frac{z}{\hbar} T_2(x, y) + f(z) T_3(x, y) \tag{8}$$

For porous FG plate the equilibrium equations are derived by using the virtual work principle, which can be written as

$$\int_{-\hbar/2}^{\hbar/2} \int_{\Omega} \left[\sigma_x \delta\varepsilon_x + \sigma_y \delta\varepsilon_y + \tau_{xy}\delta\gamma_{xy} + \tau_{yz}\delta\gamma_{yz} + \tau_{zx}\delta\gamma_{zx}\right] d\Omega dz - \int_{\Omega} (q - f_e)\delta w d\Omega = 0 \tag{9}$$

Where Ω is the top surface, q is the distributed transverse load and f_e is the density of reaction force of foundation. For the Pasternak foundation model

$$\boldsymbol{f_e = K_W w - J_1 \frac{\partial^2 w}{\partial x^2} - J_2 \frac{\partial^2 w}{\partial y^2}} \tag{10}$$

where K_W is the modulus of subgrade reaction (elastic coefficient of the foundation) and J_1 and J_2 are the shear moduli of the subgrade (shear layer foundation stiffness). If foundation is homogeneous and isotropic, we will get $J_1 = J_2 = J_0$. If the shear layer foundation stiffness is neglected, Pasternak foundation becomes a Winkler foundation.

Substituting Eqs. (7) and (10) into Eq.(13) and integrating through the thickness of the plate, Eq. (13) can be rewritten as

$$\int_{\Omega}[\boldsymbol{N_x\delta\varepsilon_x^0+N_y\delta\varepsilon_y^0+N_{xy}\delta\varepsilon_{xy}^0+M_x^b\delta k_x^b+M_y^b\delta k_y^b+M_{xy}^b\delta k_{xy}^b+M_x^s e\delta k_x^s+M_y^s\delta k_y^s}$$
$$\boldsymbol{+M_{xy}^s\delta k_y^s+M_{xy}^s\delta k_{xy}^s+S_{yz}^s\delta\gamma_{yz}^s+S_{xz}^s\delta\gamma_{xz}^s]d\Omega-\int_{\Omega}(q-f_e)(\delta w_b+\delta w_s)d\Omega=0} \quad (11)$$

The stress resultants *N, M,* and *S* are defined by:

$$\begin{Bmatrix} N_x & N_y & N_{xy} \\ M_x^b & M_y^b & M_{xy}^b \\ M_x^s & M_y^s & M_{xy}^s \end{Bmatrix} = \int_{-\hbar/2}^{\hbar/2} (\sigma_x, \sigma_y, \tau_{xy}) \begin{Bmatrix} 1 \\ z \\ f(z) \end{Bmatrix} dz$$
$$(S_{xz}^s, S_{yz}^s) = \int_{-\hbar/2}^{\hbar/2} (\tau_{xz}, \tau_{yz}) g(z) dz \quad (12)$$

Substituting Eq. (10) into Eq. (16) and integrating through the thickness of the plate, the stress resultants are given as

$$\begin{Bmatrix} N \\ M^b \\ M^s \end{Bmatrix} = \begin{bmatrix} A & B & B^s \\ A & D & D^s \\ B^s & D^s & H^s \end{bmatrix} \begin{Bmatrix} \varepsilon \\ k^b \\ k^s \end{Bmatrix} - \begin{Bmatrix} N^T \\ M^{bT} \\ M^{sT} \end{Bmatrix}, \quad \mathrm{S} = A^s \gamma \quad (13)$$

Where

$$\boldsymbol{N=\{N_x,N_y,N_{xy}\}^t,\quad M^b=\{M_x^b,M_y^b,M_{xy}^b\}^t,\quad M^s=\{M_x^s,M_y^s,M_{xy}^s\}^t}$$
$$\boldsymbol{\varepsilon=\{\varepsilon_x^0,\varepsilon_y^0,\gamma_{xy}^0\}^t,\quad k^b=\{k_x^b,k_y^b,k_{xy}^b\}^t,\quad k^s=\{k_x^s,k_y^s,k_{xy}^s\}^t}$$
$$\boldsymbol{A=\begin{bmatrix} A_{11} & A_{12} & 0 \\ A_{12} & A_{22} & 0 \\ 0 & 0 & A_{66} \end{bmatrix},\quad B=\begin{bmatrix} B_{11} & B_{12} & 0 \\ B_{12} & B_{22} & 0 \\ 0 & 0 & B_{66} \end{bmatrix},\quad D=\begin{bmatrix} D_{11} & D_{12} & 0 \\ D_{12} & D_{22} & 0 \\ 0 & 0 & D_{66} \end{bmatrix}}$$
$$\boldsymbol{B^s=\begin{bmatrix} B_{11}^s & B_{12}^s & 0 \\ B_{12}^s & B_{22}^s & 0 \\ 0 & 0 & B_{66}^s \end{bmatrix},\quad D^s=\begin{bmatrix} D_{11}^s & D_{12}^s & 0 \\ D_{12}^s & D_{22}^s & 0 \\ 0 & 0 & D_{66}^s \end{bmatrix},\quad H^s=\begin{bmatrix} H_{11}^s & H_{12}^s & 0 \\ H_{12}^s & H_{22}^s & 0 \\ 0 & 0 & H_{66}^s \end{bmatrix}}$$
$$\boldsymbol{S=\{S_{yz}^z,S_{xz}^s\}^t\ ,\quad \gamma=\{\gamma_{yz},\gamma_{xz}\}^t,\quad A^s=\begin{bmatrix} A_{44}^s & 0 \\ 0 & A_{55}^s \end{bmatrix}} \quad (14)$$

Where A_{ij}, B_{ij}, etc., are the plate stiffness, defined by

$$\boldsymbol{\begin{Bmatrix} A_{11} & B_{11} & D_{11} & B_{11}^s & D_{11}^s & H_{11}^s \\ A_{12} & B_{12} & D_{12} & B_{12}^s & D_{12}^s & H_{12}^s \\ A_{66} & B_{66} & D_{66} & B_{66}^s & D_{66}^s & H_{66}^s \end{Bmatrix} = \int_{-\square/2}^{\square/2} \frac{E(z)}{1-\nu^2} (1, z, z^2, f(z), zf(z), f^2(z)) \begin{Bmatrix} 1 \\ \nu \\ \frac{1-\nu}{2} \end{Bmatrix}} \quad (15)$$

and

$$\boldsymbol{(A_{22},B_{22},D_{22},B_{22}^s,D_{22}^s,H_{22}^s)=(A_{11},B_{11},D_{11},B_{11}^s,D_{11}^s,H_{11}^s)}$$
$$A_{44}^s=A_{55}^s=\int_{-\hbar/2}^{\hbar/2}\frac{E(z)}{2(1+\nu)}[g(z)]^2dz \quad (16)$$

The stress and moment resultants, $N_x^T=N_y^T$, $M_x^{bT}=M_y^{bT}$, $M_x^{sT}=M_y^{sT}$ due to thermal loading are defined respectively by

$$\begin{Bmatrix} N_x^T \\ M_x^{bT} \\ M_x^{sT} \end{Bmatrix} = \int_{-\hbar/2}^{\hbar/2} \frac{E(z)}{1-\nu} \alpha(z) T \begin{Bmatrix} 1 \\ z \\ f(z) \end{Bmatrix} dz \quad (17)$$

The governing equations of equilibrium can be derived from Eq. (15) by integrating the displacement gradients by parts and setting the coefficients δu_0, δv_0, δw_b and δw_s zero separately. Thus one can obtain the equilibrium equations associated with the present shear deformation theory

$$\begin{gathered}
\delta u_0\colon \ \frac{\partial N_x}{\partial x}+\frac{\partial N_{xy}}{\partial y}=0\\
\delta v_0\colon \ \frac{\partial N_{xy}}{\partial x}+\frac{\partial N_y}{\partial y}=0\\
\delta w_b\colon \ \frac{\partial^2 M_x^b}{\partial x^2}+2\frac{\partial^2 M_{xy}^b}{\partial x\partial y}+\frac{\partial^2 M_y^b}{\partial y^2}-f_e+q=0\\
\delta w_s\colon \ \frac{\partial^2 M_x^s}{\partial x^2}+2\frac{\partial^2 M_{xy}^s}{\partial x\partial y}+\frac{\partial^2 M_y^s}{\partial y^2}+\frac{\partial S_{xz}^s}{\partial x}+\frac{\partial S_{yz}^s}{\partial y}-f_e+q=0
\end{gathered} \tag{18}$$

Substituting from Eq. (17) into Eq. (21), we obtain the following equation

$$\begin{gathered}
A_{11}d_{11}u_0+A_{66}d_{22}u_0+(A_{12}+A_{66})d_{12}v_0-B_{11}d_{111}w_b-(B_{12}+2B_{66})d_{122}w_b\\
-(B_{12}^s+2B_{66}^s)d_{122}w_s-B_{11}^s d_{111}w_s=p_1
\end{gathered} \tag{19}$$

$$\begin{gathered}
A_{22}d_{22}v_0+A_{66}d_{11}v_0+(A_{12}+A_{66})d_{12}u_0-B_{22}d_{222}w_b\\
-(B_{12}+2B_{66})d_{112}w_b-(B_{12}^s+2B_{66}^s)d_{112}w_s-B_{22}^s d_{222}w_s=p_2
\end{gathered} \tag{20}$$

$$\begin{gathered}
B_{11}d_{11}u_0+(B_{12}+2B_{66})d_{122}u_0+(B_{12}+2B_{66})d_{112}v_0+B_{22}d_{222}v_0\\
-D_{11}d_{1111}w_b-2(D_{12}+2D_{66})d_{1122}w_b-D_{22}d_{2222}w_b-D_{11}^s d_{1111}w_s\\
-2(D_{12}^s+2D_{66}^s)d_{1122}w_s-D_{22}^s d_{2222}w_s=p_3
\end{gathered} \tag{21}$$

$$\begin{gathered}
B_{11}^s d_{111}u_0+(B_{12}^s+2B_{66}^s)d_{122}u_0+(B_{12}^s+2B_{66}^s)d_{112}v_0\\
+B_{22}^s d_{222}v_0-D_{11}^s d_{1111}w_b-2(D_{12}^s+2D_{66}^s)d_{1122}w_b\\
-D_{22}^s d_{2222}w_b-H_{11}^s d_{1111}w_s-2(H_{12}^s+2H_{66}^s)d_{1122}w_s\\
-H_{22}^s d_{2222}w_s+A_{55}^s d_{11}w_s+A_{44}^s d_{22}w_s=p_4
\end{gathered} \tag{22}$$

Where $\{p\}=\{p_1,p_2,p_3,p_4\}^t$ is a generalized force vector, d_{ij}, d_{ijl} and d_{ijlm} are the following differential operators

$$d_{ij}=\frac{\partial^2}{\partial x_i\partial x_j},\ \ d_{ijl}=\frac{\partial^3}{\partial x_i\partial x_j\partial x_l},\ \ d_{ijlm}=\frac{\partial^4}{\partial x_i\partial x_j\partial x_l\partial x_m},\ \ d_i=\frac{\partial}{\partial x_i},\ \ (i,j,l,m=1,2) \tag{23}$$

The components of the generalized force vector $\{p\}$ are given by

$$\begin{gathered}
p_1=\frac{\partial N_x^T}{\partial x},\\
p_2=\frac{\partial N_y^T}{\partial y},\\
p_3=f_e+q-\frac{\partial^2 M_x^{bT}}{\partial x^2}-\frac{\partial^2 M_y^{bT}}{\partial y^2},\\
p_4=f_e+q-\frac{\partial^2 M_x^{sT}}{\partial x^2}-\frac{\partial^2 M_y^{sT}}{\partial y^2}
\end{gathered} \tag{24}$$

To solve this problem, Navier presented the uniform external force and the transverse uniform temperature loads in the form of a double trigonometric series

$$\begin{Bmatrix} q \\ T_1 \end{Bmatrix}=\begin{Bmatrix} q_0 \\ t_1 \end{Bmatrix} sin(\lambda x)\, sin(\mu y),\quad (i=1,2,3) \tag{25}$$

where $\lambda = \pi/a,\ \mu = \pi/b,\ q_0$ and t_i are constants.

Clearly, the Navier solution can be assumed as

$$\begin{Bmatrix} \mu_0 \\ \nu_0 \\ w_b \\ w_s \end{Bmatrix} = \begin{Bmatrix} U\cos(\lambda x)\sin(\mu y) \\ V\sin(\lambda x)\cos(\mu y) \\ W_b\sin(\lambda x)\sin(\mu y) \\ W_s\sin(\lambda x)\sin(\mu y) \end{Bmatrix} \tag{26}$$

Where U, V, W_b and W_s are arbitrary parameters to be determined subjected to the condition that the solution in Eq. (25) satisfies governing Eq. (22). One obtains the following operator equation

$$[K]\{\Delta\} = \{P\} \tag{27a}$$

$$\begin{bmatrix} k_{11} & k_{12} & k_{13} & k_{14} \\ k_{12} & k_{22} & k_{23} & k_{24} \\ k_{13} & k_{23} & k_{33} & k_3 \\ k_{14} & k_{24} & k_{34} & k_{44} \end{bmatrix} \{\Delta\} = \{P\} \tag{27b}$$

Where $\{\Delta\} = \{U, V, W_b, W_s\}^t$ and $[K]$ is the symmetric matrix.

In which

$$\begin{aligned}
k_{11} &= -(A_{11}\lambda^2 + A_{66}\mu^2) \\
k_{12} &= -\lambda\mu(A_{12} + A_{66}) \\
k_{13} &= \lambda[B^s_{11}\lambda^2 + (B_{12} + 2B_{66})\mu^2] \\
k_{14} &= \lambda[B^s_{11}\lambda^2 + (B^s_{12} + 2B^s_{66})\mu^2] \\
k_{22} &= -(A_{66}\lambda^2 + A_{22}\mu^2) \\
k_{23} &= \mu[(B_{12} + 2B_{66})\lambda^2 + B_{22}\mu^2] \\
k_{24} &= \mu[(B^s_{12} + 2B^s_{66})\lambda^2 + B^s_{22}\mu^2] \\
k_{33} &= -(D_{11}\lambda^4 + 2(D_{12} + 2D_{66})\lambda^2\mu^2 + D_{22}\mu^4 + K_W + J_1\lambda^2 + J_2\mu^2) \\
k_{34} &= -(D^s_{11}\lambda^4 + 2(D^s_{12} + 2D^s_{66})\lambda^2\mu^2 + D^s_{22}\mu^4 + K_W + J_1\lambda^2 + J_2\mu^2) \\
k_{44} &= -(H^s_{11}\lambda^4 + 2(H^s_{11} + 2H^s_{66})\lambda^2\mu^2 + H^s_{22}\mu^4 + A^s_{55}\lambda^2 + A^s_{44}\mu^2 + K_W + J_1\lambda^2 + J_2\mu^2)
\end{aligned} \tag{28}$$

The components of the generalized force vector $\{P\} = \{P_1, P_2, P_3, P_4\}^t$ are given by

$$\begin{aligned}
P_1 &= \lambda(A^T t_1 + B^T t_2 + {}^{\alpha}B^T t_3) \\
P_2 &= \mu(A^T t_1 + B^T t_2 + {}^{\alpha}B^T t_3) \\
P_3 &= -q_0 - \hbar(\lambda^2 + \mu^2)(B^T t_1 + D^T t_2 + {}^{\alpha}D^T t_3) \\
P_4 &= -q_0 - \hbar(\lambda^2 + \mu^2)({}^{s}B^T t_1 + {}^{s}D^T t_2 + {}^{s}F^T t_3)
\end{aligned} \tag{29}$$

Where

$$\{A^T, B^T, D^T\} = \int_{-\frac{\hbar}{2}}^{\frac{\hbar}{2}} \frac{E(z)}{1-\nu}\alpha(z)\{1, \overline{z}, \overline{z}^2\}dz$$

$$\{{}^{\alpha}B^T,\ {}^{\alpha}D^T\} = \int_{-\frac{\hbar}{2}}^{\frac{\hbar}{2}} \frac{E(z)}{1-\nu}\alpha(z)f(z)\{1, \overline{z}\}dz$$

$$\{{}^{s}B^T,\ {}^{s}D^T,\ {}^{s}F^T\} = \int_{-\hbar/2}^{\hbar/2} \frac{E(z)}{1-\nu}\alpha(z)\overline{f}(z)\{1, \overline{z}, f(z)\}dz \tag{30}$$

Table 1 materials properties of functionally graded plate (Ti-6Al-4V / ZrO_2)

Materials	E	ν	α
Ti-6Al-4V	66.2 GPa	1/3	$10.3\times(10^{-6}/C°)$.
ZrO_2	117.0 GPa	1/3	$7.11\times(10^{-6}/C°)$.

Table 2 Effect of the porosity on the dimensionless deflection $\widehat{w}$ of square plates (a=10h, b=a, q_0=100, T_1=T_3=0, T_2=0)

k	Theory	Porosity	$\widehat{w}$
2	Thai H-T *et al.*	β=0	0.3737
	Taibi *et al.*	β=0	0.3734
	Present	β=0	0.3795406
		β=0.1	0.4278580
		β=0.2	0.4909164
5	Thai H-T *et al.*	β=0	0.4101
	Taibi *et al.*	β=0	0.4094
	Present	β=0	0.4036893
		β=0.1	0.4581206
		β=0.2	0.5300833
10	Thai H-T *et al.*	β=0	0.3988
	Taibi *et al.*	β=0	0.4178
	Present	β=0	0.4234319
		β=0.1	0.4829429
		β=0.2	0.5622425

In which

$$\overline{z} = z/\hbar,\ \overline{f}(z) = f(z)/\hbar \tag{31}$$

3. Results and discussions

The procedure outlined in the previous sections is used here to analyze the thermo-mechanical effect on the bending of porous functionally graded plates resting on Winkler-Pasternak foundations. A comparison study is presented between the results of the present study and those given by Bouderba (2013), Thai H-T (2014), Taibi (2015). Here, Titanium, Ti-6Al-4V, and Zirconia, ZrO_2 are used as the metal and ceramic constituents. The material properties of the used FGM's are listed in Table 1. For all the computations, the Poisson's ratio is taken as 0.3 and the reference temperature is taken by T_0=25°C (room temperature).

Table 2 presents the comparison study of dimensionless deflection $\widehat{w}$of square plates subjected to mechanical loading. These two comparisons show that the results presented when β≠0 are in good agreement with existing results. The results show that the porosity has a significant effect on the dimensionless deflection of FG plate.

Tables 3 and 4 present the effect of the volume fraction exponent and elastic foundation parameters on the dimensionless and stresses of an FG rectangular plate with porosities. Temperature

Table 3 Effect of the porosity and volume fraction exponent on the dimensionless and stresses of an FG rectangular plate (a=10h, b=2a, q_0=100, T=0, K_0=100, J_0=100)

k	Theory	Porosity	$\overline{w}$	$\overline{\sigma_x}$	$\overline{\tau_{xz}}$
ceramic	Bouderba (2013)	β=0	0.077197	0.048071	-0.044643
	PSDT	β=0	0.077197	0.048050	-0.043259
	TSDT	β=0	0.077197	0.048071	-0.044643
	Present	β=0	0.077195	0.047277	-0.04423
		β=0.1	0.077886	0.043968	-0.04113
		β=0.2	0.078589	0.040598	-0.03798
2	Bouderba (2013)	β=0	0.079758	0.044595	-0.032215
	PSDT	β=0	0.079758	0.044574	-0.031170
	TSDT	β=0	0.079758	0.044595	-0.032215
	Present	β=0	0.079756	0.043748	-0.03190
		β=0.1	0.080519	0.040129	-0.02847
		β=0.2	0.081304	0.036395	-0.024945
5	Bouderba (2013)	β=0	0.080150	0.045736	-0.029922
	PSDT	β=0	0.080150	0.045714	-0.028921
	TSDT	β=0	0.080150	0.045736	-0.029922
	Present	β=0	0.080149	0.044821	-0.02962
		β=0.1	0.080910	0.041156	-0.026179
		β=0.2	0.081693	0.037354	-0.022645
metal	Bouderba (2013)	β=0	0.081190	0.050559	-0.026565
	PSDT	β=0	0.081191	0.050538	-0.025744
	TSDT	β=0	0.081190	0.050559	-0.026565
	Present	β=0	0.081189	0.050545	-0.026318
		β=0.1	0.081954	0.024470	-0.022890
		β=0.2	0.082733	0.020736	-0.019397

elevation is ignored (T=0) in only Table 1, and side-to-thickness ratio is set equal to a/h=10. It is seen that the results of this study are in excellent agreement with the results of Bouderba (2013) when β=0 and take different values when β≠0. As the FG plate becomes richer on metal, the dimensionless and the stresses of the FG plate increase when (T=0) and decrease when (T≠0). Table 5 shows the effect of the volume fraction of the porosity on the dimensionless deflection $\hat{w}$ of an FG square plate (b=a) resting on the elastic foundation and subjected to a thermo-mechanical loading. It can be seen that the dimensionless deflection decrease as the side-to-thickness ratio increase (thin plate).

Tables 6 and 7 show the effect of the volume fraction of the porosity, volume fraction exponent, and elastic foundation parameters on the dimensionless center deflection $\hat{w}$ of an porous FG plate subjected to mechanical and thermo-mechanical loading, respectively. The side-to-thickness ratio is taken to be a/h=10. It can be seen that the dimensionless center deflection of the porous FG plate decreases with an increase in foundation stiffness, but increases with an increase in the volume fraction of the porosity and the volume fraction exponent. Compared to the Winkler parameter K_0, the Pasternak foundation parameter J_0 has a dominant effect on decreasing the dimensionless center deflection.

Table 4 Effect of the porosity and volume fraction exponent on the dimensionless and stresses of an FG rectangular plate (a=10h, b=2a, q_0=100, T_1=T_3=0, T_2=10, K_0=100, J_0=100)

k	Theory	Porosity	$\overline{w}$	$\overline{\sigma_x}$	$\overline{\tau_{xz}}$
ceramic	Bouderba (2013)	β=0	0.17270	-0.50052	0.38756
	PSDT	β=0	0.17270	-0.50034	0.37555
	TSDT	β=0	0.17270	-0.50052	0.38756
	Present	β=0	0.17269	-0.49364	0.3839
		β=0.1	0.16669	-0.45837	0.3571
		β=0.2	0.16059	-0.42263	0.3297
2	Bouderba (2013)	β=0	0.16819	-0.48398	0.35985
	PSDT	β=0	0.16819	-0.48375	0.34801
	TSDT	β=0	0.16819	-0.48398	0.35985
	Present	β=0	0.16817	-0.47455	0.3563
		β=0.1	0.15957	-0.43542	0.3174
		β=0.2	0.15071	-0.39501	0.2775
5	Bouderba (2013)	β=0	0.16719	-0.48223	0.34986
	PSDT	β=0	0.16720	-0.48201	0.33789
	TSDT	β=0	0.16719	-0.48223	0.34986
	Present	β=0	0.16719	-0.47156	0.3462
		β=0.1	0.15822	-0.43329	0.3055
		β=0.2	0.14902	-0.39350	0.26367

Table 5 Effects of the porosity and side-to-thickness ratio on the dimensionless deflection $\hat{w}$ of an FG square plate (b=a, q_0=100, T_1=T_3=0, T_2=10, K_0=100, J_0=100)

k	Theory	Porosity	a/h			
			5	10	20	50
ceramic	Bouderba (2013)	β=0	0.53445	0.18171	0.077180	0.046508
	Present	β=0	0.53496	0.18171	0.077181	0.046507
		β=0.1	0.50155	0.17273	0.075238	0.046622
		β=0.2	0.46741	0.16354	0.073262	0.046738
2	Bouderba (2013)	β=0	0.49953	0.17443	0.076803	0.048043
	Present	β=0	0.50013	0.17445	0.076800	0.048045
		β=0.1	0.45280	0.16139	0.073856	0.048053
		β=0.2	0.40400	0.14789	0.070794	0.048061
5	Bouderba (2013)	β=0	0.48761	0.17256	0.076639	0.048259
	Present	β=0	0.48835	0.17257	0.076638	0.048259
		β=0.1	0.43872	0.15895	0.073531	0.048243
		β=0.2	0.38789	0.14489	0.070344	0.048229

Dimensionless deflection $\hat{w}$ of a square FG plate is presented in Table 8 for different values of thickness ratio a/h, power-law index k, and foundation parameters (K_0, J_0). The obtained results are compared with those given by Taibi (2015) for the perfect FG plate (β=0). It can be concluded that the volume fraction of the porosity has a significant effect on the dimensionless deflection $\hat{w}$ of a square FG plate resting on the Pasternak or Winkler-Pasternak foundations

Table 6 Effect of porosity and elastic foundation parameters on the dimensionless center deflection $\hat{w}$ of an FG square plate subjected to mechanical loading (a=10h, b=a, q_0=100, T_1=T_2=T_3 =0)

k	Theory	Porosity	K_0=0, J_0=0	K_0=100, J_0=0	K_0=0, J_0= 100	K_0=100, J_0=100
0	Taibi (2015)	β=0	0.6813082	0.4052251	0.08365248	0.07719493
	Present	β=0	0.6812934	0.4052198	0.08365225	0.07719474
		β=0.1	0.7391629	0.4250108	0.08446419	0.07788565
		β=0.2	0.8077758	0.4468341	0.08529205	0.07858903
2	Taibi (2015)	β=0	1.109938	0.5260525	0.08781631	0.08072715
	Present	β=0	0.9507665	0.4873809	0.08666835	0.07975602
		β=0.1	1.071814	0.5173312	0.08756987	0.08051885
		β=0.2	1.229831	0.5515355	0.08849891	0.08130363
5	Taibi (2015)	β=0	1.181016	0.5414982	0.08823646	0.08108206
	Present	β=0	1.009736	0.5024222	0.08713221	0.08014868
		β=0.1	1.145591	0.5339279	0.08803308	0.08091029
		β=0.2	1.325117	0.5699143	0.08895923	0.08169198

Table 7 Effect of porosity and elastic foundation parameters on the dimensionless center deflection $\hat{w}$ of an FG plate subjected to thermo-mechanical loading (a=10h, b=2a, q_0=100, T_1=T_3=0, T_2=10)

k	Theory	Porosity	K_0=0, J_0=0	K_0=100, J_0=0	K_0=0, J_0= 100	K_0=100, J_0=100
0	Taibi (2015)	β=0	1.524169	0.9065374	0.1871406	0.1726943
	Present	β=0	1.524154	0.9065366	0.1871425	0.1726961
		β=0.1	1.582024	0.9096466	0.1807779	0.1666979
		β=0.2	1.650637	0.9130758	0.1742886	0.1605915
2	Taibi (2015)	β=0	2.288283	1.084526	0.1810449	0.1664296
	Present	β=0	2.004883	1.027741	0.1827577	0.1681818
		β=0.1	2.124061	1.025218	0.1735411	0.1595679
		β=0.2	2.279672	1.022352	0.1640458	0.1507082
5	Taibi (2015)	β=0	2.394417	1.097845	0.1788923	0.1643874
	Present	β=0	2.106337	1.048066	0.1817601	0.1671923
		β=0.1	2.240229	1.044108	0.1721507	0.1582219
		β=0.2	2.417239	1.039620	0.1622767	0.1490200

To illustrate the effect of temperature parameters (T_2) on the bending responses of FG plates, Table 9 shows the results of the dimensionless and stresses of an FG rectangular plate subjected to mechanical and thermo-mechanical loading. It can be observed that the dimensionless and stresses increase when the volume fraction of the porosity increase for both mechanical and thermo-mechanical loading.

Table 10 present the effect of the distribution shape of the porosity on the dimensionless and stresses of an FG plate subjected to a thermomechanical loading. Both even distribution and uneven distribution of porosity are taken into account. From this table, it was found that the distribution shape of porosity significantly influences on the thermo-mechanical behavior of FG plates, in terms of deflection and stresses.

Table 8 Effect of porosity and elastic foundation parameters on the dimensionless center deflection $\hat{w}$ of an FG square plate subjected to thermo-mechanical loading ($b=a$, $q_0=100$, $T_1=0$, $T_2=T_3=10$)

k	Theory	Porosity	$K_0=0$, $J_0=100$			$K_0=100$, $J_0=100$		
			$a/h=5$	$a/h=10$	$a/h=20$	$a/h=5$	$a/h=10$	$a/h=20$
1	SPT	$\beta=0$	0.5464189	0.1850845	0.08088404	0.5226103	0.1771234	0.07741799
	HPT	$\beta=0$	0.5459374	0.1850501	0.08088214	0.5221480	0.1770903	0.07741611
	Taibi (2015)	$\beta=0$	0.5456821	0.1850325	0.08088109	0.5219026	0.1770732	0.07741516
	Present	$\beta=0$	0.5374418	0.1850155	0.08059350	0.5142352	0.1771592	0.07718862
		$\beta=0.1$	0.4908725	0.1722699	0.07775425	0.4694427	0.1648617	0.07442569
		$\beta=0.2$	0.4429306	0.1590929	0.07481506	0.4233768	0.1521627	0.07156912
2	SPT	$\beta=0$	0.5288591	0.1804318	0.08005720	0.5056076	0.1725899	0.07658943
	HPT	$\beta=0$	0.5282195	0.1803852	0.08005454	0.5049920	0.1725450	0.07658675
	Taibi (2015)	$\beta=0$	0.5278306	0.1803571	0.08005289	0.5046192	0.1725179	0.07658525
	Present	$\beta=0$	0.5228637	0.1822373	0.08021888	0.5001213	0.1744407	0.07680412
		$\beta=0.1$	0.4736050	0.1687084	0.07718506	0.4527749	0.1613975	0.07385538
		$\beta=0.2$	0.4227992	0.1546860	0.07403606	0.4039917	0.1478945	0.07079844

Table 9 Effect of the porosity volume fraction exponent on the dimensionless and stresses of an FG rectangular plate subjected to mechanical and thermo-mechanical loading ($a=10h$, $b=2a$, $q_0=100$, $T_1=T_3=0$, $K_0=0$, $J_0=0$)

T_2	Theory	Porosity	$\overline{w}$	$\overline{\sigma_x}$
0	Bouderba (2013)	$\beta=0$	0.68131	0.42424
	PSDT	$\beta=0$	0.68134	0.42408
	TSDT	$\beta=0$	0.68131	0.42424
	Present	$\beta=0$	0.68129	0.41725
		$\beta=0.1$	0.73917	0.41726
		$\beta=0.2$	0.80778	0.41730
10	Bouderba (2013)	$\beta=0$	1.5241	0.34104
	PSDT	$\beta=0$	1.5243	0.34091
	TSDT	$\beta=0$	1.5241	0.34104
	Present	$\beta=0$	1.5241	0.33410
		$\beta=0.1$	1.5820	0.34060
		$\beta=0.2$	1.6507	0.34710

Fig. 2 aims to analyze the influence of the volume fraction of the porosity on the dimensionless center deflection of an FGM square plate subjected to thermo-mechanical loading. The gradient index is taken to be $k=2$. It can be observed that the dimensionless deflection decreases when the foundation parameters K_0, J_0 increase, and the Winkler foundation parameter K_0 has more effect on reducing the dimensionless deflection than the Pasternak parameter J_0. Such behavior is because the inclusion of foundation parameters will increase the stiffness of the plate, and thus, lead to a reduction of deflection. It is also observed from these figures that the volume fraction of the porosity has more effect when the plate reposed on the Winkler-Pasternak foundation. Fig. 3 shows the effect of the porosity on the dimensionless center deflection through the aspect ratio of an FGM plate subjected to thermo-mechanical loading. The side-to-thickness ratio is taken to be $a/h=10$, and the volume fraction index is taken to be $k=2$. It can be seen that the dimensionless center deflection

Table 10 Effect of the distribution shape of the porosity on the dimensionless and stresses of an FG rectangular plate (a=10h, b=2a, q_0=100, T_1=0, T_2= T_3=10, K_0=100, J_0=100)

a/h	k	Porosity	$\overline{w}$		$\overline{\sigma_x}$		$\overline{\tau_{xz}}$	
			Even	Uneven	Even	Uneven	Even	Uneven
5	0	β=0	0.6967	0.6967	- 0.5916	- 0.5916	1.3729	1.3729
		β=0.1	0.6536	0.6832	-0.5506	-0.5893	1.2756	1.3062
		β=0.2	0.6097	0.6695	-0.5087	-0.5864	1.1768	1.2368
	2	β=0	0.6497	0.6497	-0.5277	-0.5277	1.2406	1.2406
		β=0.1	0.5894	0.6304	-0.4821	-0.5191	1.1043	1.1468
		β=0.2	0.5278	0.6105	-0.4348	-0.5087	0.96458	1.0470
	5	β=0	0.6366	0.6366	-0.5082	-0.5082	1.1918	1.1918
		β=0.1	0.5738	0.6158	-0.4642	-0.4977	1.0489	1.0872
		β=0.2	0.5097	0.5941	-0.4176	-0.4848	0.9027	0.9742
10	0	β=0	0.2465	0.2465	-0.6480	-0.6480	0.7207	0.7207
		β=0.1	0.2354	0.2435	-0.6035	-0.6484	0.6701	0.6878
		β=0.2	0.2240	0.2404	-0.5580	-0.6492	0.6187	0.6534
	2	β=0	0.2365	0.2365	-0.6107	-0.6107	0.6613	0.6613
		β=0.1	0.2206	0.2320	-0.5594	-0.6072	0.5891	0.6141
		β=0.2	0.2043	0.2275	-0.5056	-0.6027	0.5149	0.5637
	5	β=0	0.2343	0.2343	-0.6070	-0.6070	0.6407	0.6407
		β=0.1	0.2178	0.2295	-0.5572	-0.6034	0.5651	0.5881
		β=0.2	0.2008	0.2247	-0.5046	-0.5986	0.4875	0.5308
20	0	β=0	0.1203	0.1203	-0.5262	-0.5262	0.3014	0.3014
		β=0.1	0.1180	0.1197	-0.4905	-0.5275	0.2803	0.2878
		β=0.2	0.1156	0.1190	-0.4538	-0.5287	0.2588	0.2737
	2	β=0	0.1197	0.1197	-0.5067	-0.5067	0.2904	0.2904
		β=0.1	0.1163	0.1188	-0.4642	-0.5053	0.2586	0.2699
		β=0.2	0.1127	0.1178	-0.4194	-0.5031	0.2260	0.2481
	5	β=0	0.1195	0.1195	-0.5041	-0.5041	0.2839	0.2839
		β=0.1	0.1159	0.1185	-0.4633	-0.5032	0.2505	0.2609
		β=0.2	0.1122	0.1175	-0.4200	-0.5016	0.2161	0.2359

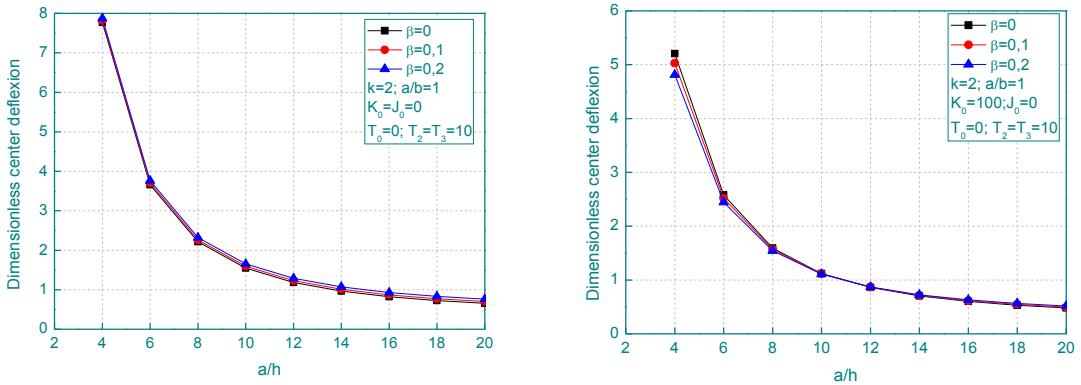

Fig. 2 Effect of the porosity on the dimensionless center deflection through side-to thickness ratio of an FGM square plate subjected to thermo-mechanical loading

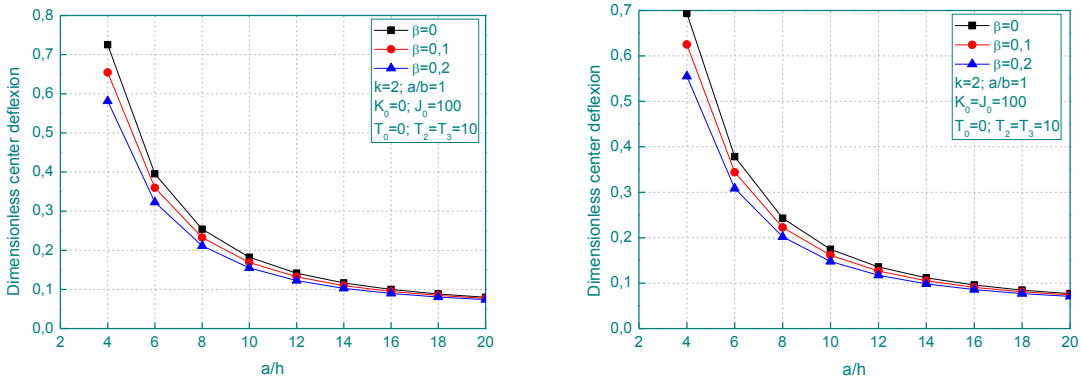

Fig. 2 Continued

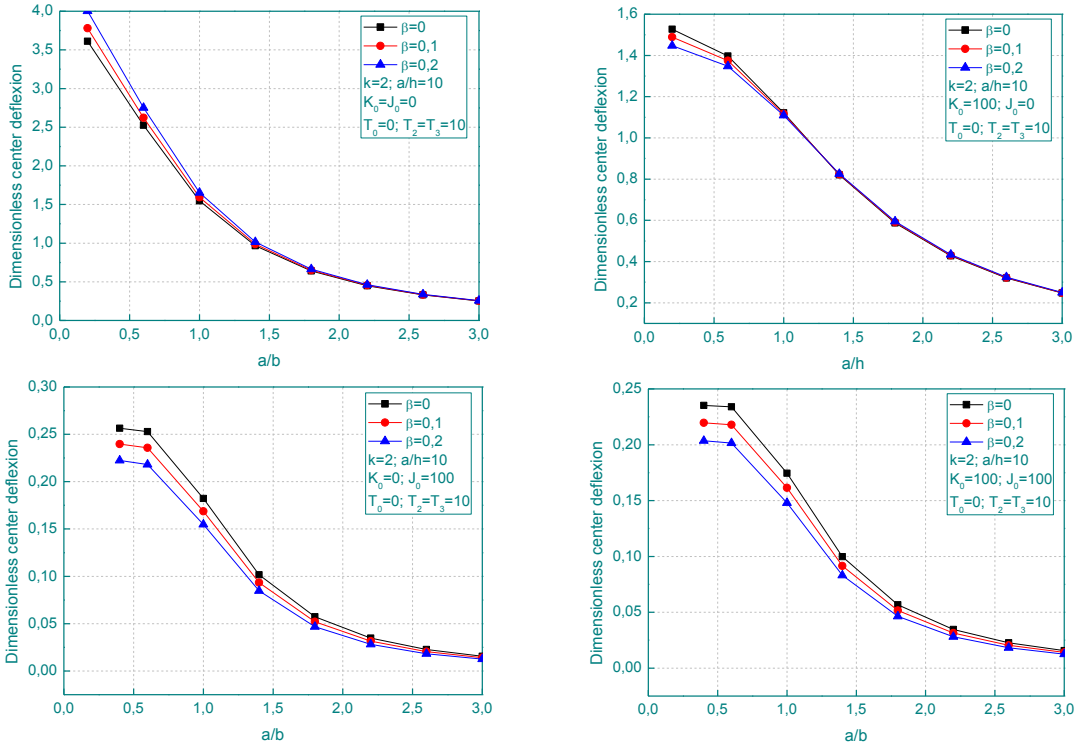

Fig. 3 Effect of the porosity on the dimensionless center deflection through the aspect ratio of an FGM plate subjected to thermo-mechanical loading

decrease when the aspect ratio *a/b* increase. The results show that the imperfect FGM plate ($\beta \neq 0$) will undergo small deflections when the plate is reposed on the elastic foundation.

Fig. 4 present the variation of the dimensionless axial stress through the thickness of an FGM rectangular plate containing porosities and subjected to thermo-mechanical loading. The side-to-thickness ratio is taken to be $a/h=10$, and the aspect ratio is taken to be $b=2a$. it can be concluded that the volume fraction of porosity influences the variation of the dimensionless axial stress through

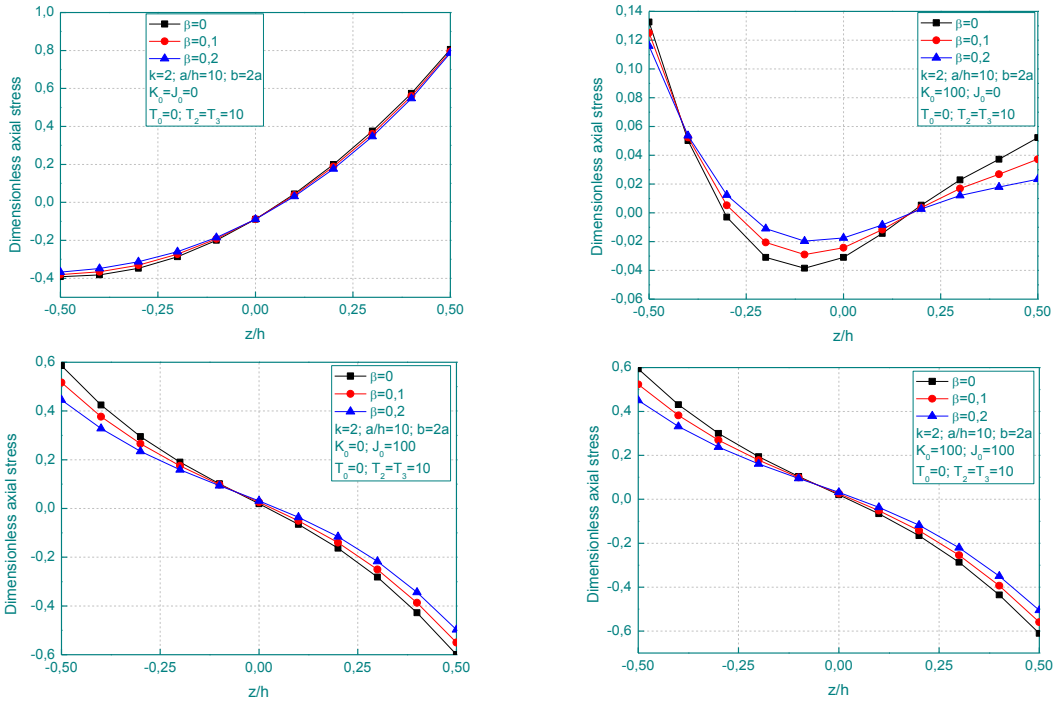

Fig. 4 Effect of the porosity on the dimensionless axial stress through the thickness of an FGM rectangular plate subjected to thermo-mechanical loading

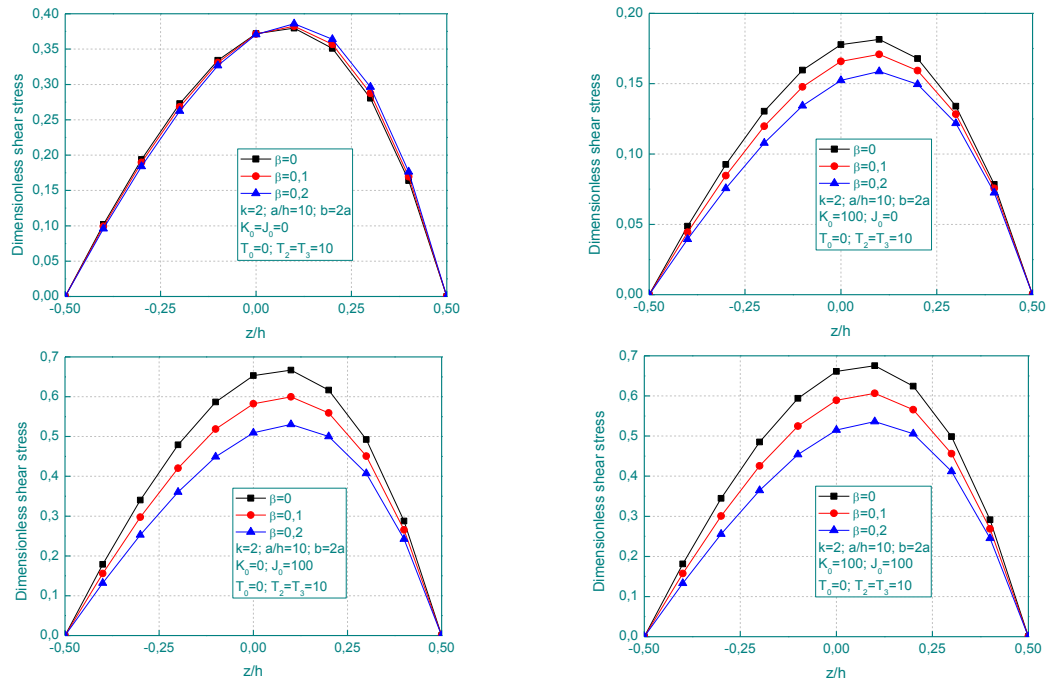

Fig. 5 Effect of the porosity on the dimensionless shear stress through the thickness of an FGM rectangular plate subjected to thermo-mechanical loading

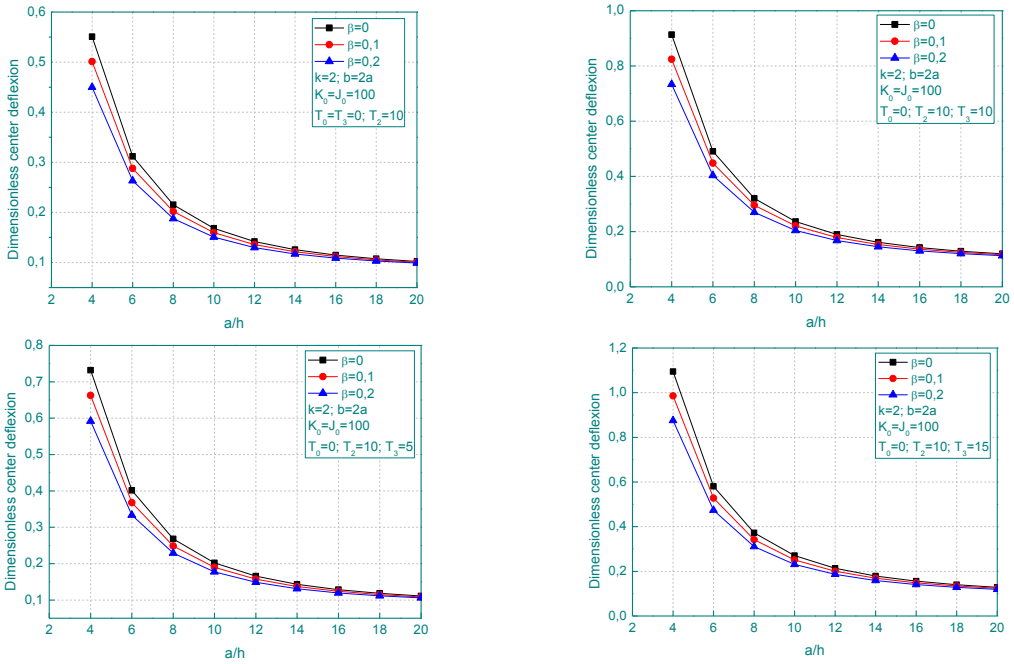

Fig. 6 Effect of the porosity and the thermal loading on the dimensionless center deflection through side-to thickness ratio of an FGM rectangular plate subjected to thermo-mechanical loading

the thickness. It can also be seen that the dimensionless axial stresses are tensile at the top surface and compressive at the bottom surface when (K_0=0, J_0=0) and becomes compressive at the top surface and tensile at the bottom surface when the FGM plate reposed on an elastic foundation.

Fig. 5 shows the through-the-thickness variation of dimensionless shear stress of an FGM rectangular plate subjected to thermo-mechanical loading. It can be observed easily from the figure that the volume fraction of the porosity provides a greater influence on dimensionless shear stress when the FGM plate reposed on an elastic foundation. It is also seen from the figure that, increasing the value of the volume fraction of the porosity β decreases the dimensionless shear stress. In addition, it can be seen that the shear stiffness coefficient J_0 increases the dimensionless shear stress, in contrast, Winkler coefficient K_0 decreases it.

To examine the influence of the thermal loading on the dimensionless center deflection of an FGM rectangular plate with porosities reposed on the Winkler-Pasternak foundation, the variation of the dimensionless center deflection of Ti-6Al-4V / ZrO_2 FG plate is displayed in Fig. 6 versus the side-to-thickness ratio. The main conclusion of Fig. 6 is that increasing the thermal loading increases the dimensionless center deflection.

5. Conclusions

This paper presents an analytical solution for thermo-mechanical bending of FG plates containing porosities and resting on elastic foundation using a new refined hyperbolic shear deformation plate theory. The variation of distribution shape of porosity is described using the modified power-law

distribution for two material constitutions with porosity. The governing equations are solved easily by using Navier's solutions. The dimensionless center deflections as well as the stresses obtained are compared with others and a very good agreement has been found which proves the precision of the method. In accordance with numerical and graphical results, some conclusions can be drawn as follows:

- The porosity distribution in the functionally graded materials has a significant effect on the dimensionless center deflection and stresses of FGM plate subjected to thermo-mechanical loading .
- The dimensionless deflection decreases when the foundation parameters K0, J0 increase, and the Winkler foundation parameter K0 has more effect on reducing the dimensionless deflection than the Pasternak parameter J0.
- Increasing value of the volume fraction of the porosity β decreases the dimensionless shear stress.
- The results show that the imperfect FGM plate ($\beta \neq 0$) will undergo small deflections when the plate reposed on the elastic foundation.
- Increasing thermal loading increases the dimensionless center deflection.
- The uneven distribution of porosity has more effect on increasing the dimensionless deflection and stresses than the even distribution of the porosity when the FG plate reposed on the elastic foundations.

Acknowledgments

This research was supported by the Algerian Ministry of Higher Education and Scientific Research (MESRS) as part of the grant for the PRFU research project n° A01L02UN140120200002 and by the University of Tiaret, in Algeria.

References

Abdelhak, Z., Hadji, L., Daouadji, T.H. and Adda Bedia, E.A. (2016), "Thermal buckling response of functionally graded sandwich plates with clamped boundary conditions", *Smart Struct. Syst.*, **18**(2), 267-291. https://doi.org/10.12989/sss.2016.18.2.267.

Abdelhak, Z., Hadji, L., Khelifa, Z., Hassaine Daouadji, T. and Adda Bedia, E.A. (2016), "Analysis of buckling response of functionally graded sandwich plates using a refined shear deformation theory", *Wind Struct.*, **22**(3), 291-305. https://doi.org/10.12989/was.2016.22.3.291.

Adim, B. and Daouadji, T.H. (2016), "Effects of thickness stretching in FGM plates using a quasi-3D higher order shear deformation theory", *Adv. Mater. Res.*, **5**(4), 223. https://doi.org/10.12989/amr.2016.5.4.223.

Adim, B., Daouadji, T.H. and Abbes, B. (2016), "Buckling analysis of anti-symmetric cross-ply laminated composite plates under different boundary conditions", *Int. Appl. Mech.*, **52**(6), 661-676. https://doi.org/10.1007/s10778-016-0787-x.

Adim, B., Daouadji, T.H., Abbes, B. and Rabahi, A. (2016), "Buckling and free vibration analysis of laminated composite plates using an efficient and simple higher order shear deformation theory", *Mech. Indus.*, **17**(5), 512. https://doi.org/10.1051/meca/2015112.

Adim, B., Daouadji, T.H., Rabia, B. and Hadji, L. (2016), "An efficient and simple higher order shear deformation theory for bending analysis of composite plates under various boundary conditions", *Earthq. Struct.*, **11**(1), 63-82. https://doi.org/10.12989/eas.2016.11.1.063.

Babaei, H., Kiani, Y. and Eslami, M.R. (2018), "Geometrically nonlinear analysis of functionally graded shallow curved tubes in thermal environment", *Thin Wall. Struct.*, **132**, 48-57. https://doi.org/10.1016/j.tws.2018.08.008.

Banh, T.T., Shin, S. and Lee, D. (2018), "Topology optimization for thin plate on elastic foundations by using multi-material", *Steel Compos. Struct.*, **27**(2), 177-184. https://doi.org/10.12989/scs.2018.27.2.177.

Belkacem, A., Tahar, H.D., Abderrezak, R., Amine, B.M., Mohamed, Z. and Boussad, A. (2018), "Mechanical buckling analysis of hybrid laminated composite plates under different boundary conditions", *Struct. Eng. Mech.*, **66**(6), 761-769. https://doi.org/10.12989/sem.2018.66.6.761.

Benachour, A., Tahar, H.D., Atmane, H.A., Tounsi, A. and Ahmed, M.S. (2011), "A four variable refined plate theory for free vibrations of functionally graded plates with arbitrary gradient", *Compos. Part B: Eng.*, **42**(6), 1386-1394. https://doi.org/10.1016/j.compositesb.2011.05.032.

Benferhat, R., Daouadji, T.H. and Adim, B. (2016), "A novel higher order shear deformation theory based on the neutral surface concept of FGM plate under transverse load", *Adv. Mater. Res.*, **5**(2), 107. https://doi.org/10.12989/amr.2016.5.2.107.

Benferhat, R., Daouadji, T.H. and Mansour, M.S. (2015), "A higher order shear deformation model for bending analysis of functionally graded plates", *Tran. Ind. Inst. Metal.*, **68**(1), 7-16. https://doi.org/10.1007/s12666-014-0428-1.

Benferhat, R., Daouadji, T.H. and Mansour, M.S. (2016), "Free vibration analysis of FG plates resting on an elastic foundation and based on the neutral surface concept using higher-order shear deformation theory", *Comptes Rendus Mecanique*, **344**(9), 631-641. https://doi.org/10.1016/j.crme.2016.03.002.

Benferhat, R., Daouadji, T.H., Mansour, M.S. and Hadji, L. (2016), "Effect of porosity on the bending and free vibration response of functionally graded plates resting on Winkler-Pasternak foundations", *Earthq. Struct.*, **10**(6), 1429-1449. https://doi.org/10.12989/eas.2016.10.6.1429.

Benferhat, R., Hassaine Daouadji, T., Hadji, L. and Said Mansour, M. (2016), "Static analysis of the FGM plate with porosities", *Steel Compos. Struct.*, **21**(1), 123-136. https://doi.org/10.12989/scs.2016.21.1.123.

Benhenni, M.A., Daouadji, T.H., Abbes, B., Abbes, F., Li, Y. and Adim, B. (2019), "Numerical analysis for free vibration of hybrid laminated composite plates for different boundary conditions", *Struct. Eng. Mech.*, **70**(5), 535-549. https://doi.org/10.12989/sem.2019.70.5.535.

Benhenni, M.A., Daouadji, T.H., Abbes, B., Adim, B., Li, Y. and Abbes, F. (2018), "Dynamic analysis for anti-symmetric cross-ply and angle-ply laminates for simply supported thick hybrid rectangular plates", *Adv. Mater. Res.*, **7**(2), 119. https://doi.org/10.12989/amr.2018.7.2.119.

Bouderba, B. (2018), "Bending of FGM rectangular plates resting on non-uniform elastic foundations in thermal environment using an accurate theory", *Steel Compos. Struct.*, **27**(3), 311-325. https://doi.org/10.12989/scs.2018.27.3.311.

Bouderba, B., Houari, M.S.A. and Tounsi, A. (2013), "Thermomechanical bending response of FGM thick plates resting on Winkler-Pasternak elastic foundations", *Steel Compos. Struct.*, **14**(1), 85-104. https://doi.org/10.12989/scs.2013.14.1.085.

Daouadj, T. H. and Adim, B. (2017), "Mechanical behaviour of FGM sandwich plates using a quasi-3D higher order shear and normal deformation theory", *Struct. Eng. Mech.*, **61**(1), 49-63. http://dx.doi.org/10.12989/sem.2017.61.1.049.

Daouadji, T.H. (2016), "Theoretical analysis of composite beams under uniformly distributed load", *Adv. Mater. Res.*, **5**(1), 1. https://doi.org/10.12989/amr.2016.5.1.001.

Daouadji, T.H. and Adim, B. (2016), "An analytical approach for buckling of functionally graded plates", *Adv. Mater. Res.*, **5**(3), 141. https://doi.org/10.12989/amr.2016.5.3.141.

Daouadji, T.H. and Benferhat, R. (2016), "Bending analysis of an imperfect FGM plates under hygro-thermo-mechanical loading with analytical validation", *Adv. Mater. Res.*, **5**(1), 35. https://doi.org/10.12989/amr.2016.5.1.035.

Daouadji, T.H. and Tounsi, A. (2013), "A new higher order shear deformation model for static behavior of functionally graded plates", *Adv. Appl. Math. Mech.*, **5**(3), 351-364. https://doi.org/10.1017/S2070073300002721.

Daouadji, T.H., Benferhat, R. and Adim, B. (2016), "Bending analysis of an imperfect advanced composite

plates resting on the elastic foundations", *Coupl. Syst. Mech.*, **5**(3), 269-283. https://doi.org/10.12989/csm.2017.5.3.269.

Daouadji, T.H., Hadj Henni, A., Tounsi, A. and El Abbes, A.B. (2012), "A new hyperbolic shear deformation theory for bending analysis of functionally graded plates", *Model. Simul. Eng.*, 2012. https://doi.org/10.1155/2012/159806.

Daouadji, T.H., Henni, A.H., Tounsi, A. and El Abbes, A.B. (2013), "Elasticity solution of a cantilever functionally graded beam", *Appl. Compos. Mater.*, **20**(1), 1-15. https://doi.org/10.1007/s10443-011-9243-6.

Demirhan, P.A. and Taskin, V. (2019), "Bending and free vibration analysis of Levy-type porous functionally graded plate using state space approach", *Compos. Part B: Eng.*, **160**, 661-676. https://doi.org/10.1016/j.compositesb.2018.12.020.

Esfahani, S.E., Kiani, Y. and Eslami, M.R. (2013), "Non-linear thermal stability analysis of temperature dependent FGM beams supported on non-linear hardening elastic foundations", *Int. J. Mech. Sci.*, **69**, 10-20. https://doi.org/10.1016/j.ijmecsci.2013.01.007.

Hadj, B., Rabia, B. and Daouadji, T.H. (2019), "Influence of the distribution shape of porosity on the bending FGM new plate model resting on elastic foundations", *Struct. Eng. Mech.*, **72**(1), 61-70. https://doi.org/10.12989/sem.2019.72.1.061.

Hadji, L., Daouadji, T.H., Tounsi, A. and Bedia, E.A. (2014), "A higher order shear deformation theory for static and free vibration of FGM beam", *Steel Compos. Struct.*, **16**(5), 507-519. http://dx.doi.org/10.12989/scs.2014.16.5.507.

Hadji, L., Khelifa, Z., Daouadji, T.H. and Bedia, E.A. (2015), "Static bending and free vibration of FGM beam using an exponential shear deformation theory", *Coupl. Syst. Mech.*, **4**(1), 99-114. http://dx.doi.org/10.12989/csm.2015.4.1.099.

Heshmati, M. and Daneshmand, F. (2019), "Vibration analysis of non-uniform porous beams with functionally graded porosity distribution", *Proc. Inst. Mech. Eng., Part L: J. Mater.: Des. Appl.*, **233**(8), 1678-1697. https://doi.org/10.1177/1464420718780902.

Isavand, S., Bodaghi, M., Shakeri, M. and Mohandesi, J.A. (2015), "Dynamic response of functionally gradient austenitic-ferritic steel composite panels under thermo-mechanical loadings", *Steel Compos. Struct.*, **18**(1), 1-28. https://doi.org/10.12989/scs.2015.18.1.001.

Joshan, Y.S., Grover, N. and Singh, B.N. (2018), "Assessment of non-polynomial shear deformation theories for thermo-mechanical analysis of laminated composite plates", *Steel Compos. Struct.*, **27**(6), 761-775. https://doi.org/10.12989/.2018.27.6.761.

Koizumi, M. (1993), "The concept of FGM", *Ceram Tran, Funct Grad Mater*., **34**, 3-10.

Liu, P., Bui, T.Q., Zhu, D., Yu, T.T., Wang, J.W., Yin, S.H. and Hirose, S. (2015), "Buckling failure analysis of cracked functionally graded plates by a stabilized discrete shear gap extended 3-node triangular plate element", *Compos. Part B: Eng.*, **77**, 179-193. https://doi.org/10.1016/j.compositesb.2015.03.036.

Moreno, D., Fernández, M. and Esquivias, P.M. (2017), "A comparison of closed-form and finite-element solutions for heat transfer in a nearly horizontal, unglazed flat plate PVT water collector: Performance assessment", *Solar Energy*, **141**, 11-24. https://doi.org/10.1007/s11029-019-09803-2.

Pakar, I., Bayat, M. and Cveticanin, L. (2018), "Nonlinear vibration of unsymmetrical laminated composite beam on elastic foundation", *Steel Compos. Struct.*, **26**(4), 453-461. https://doi.org/10.12989/scs.2018.26.4.453.

Pandey, S. and Pradyumna, S. (2017), "Stress analysis of functional graded sandwich beams subjected to thermal shock", *Procedia Eng.*, **173**, 837-843. https://doi.org/10.1016/j.proeng.2016.12.121.

Pasternak, P.L. (1954), "On a new method of analysis of an elastic foundation by means of two foundation constants", *Gosuedarstvennoe Izadatelstvo Literatim po Stroitelstvu i Arkhitekture*, **1**, 1-56.

Rabia, B., Abderezak, R., Daouadji, T.H., Abbes, B., Belkacem, A. and Abbes, F. (2018), "Analytical analysis of the interfacial shear stress in RC beams strengthened with prestressed exponentially-varying properties plate", *Adv. Mater. Res.*, **7**(1), 29. https://doi.org/10.12989/amr.2018.7.1.029.

Rabia, B., Daouadji, T.H. and Abderezak, R. (2019), "Effect of distribution shape of the porosity on the interfacial stresses of the FGM beam strengthened with FRP plate", *Earthq. Struct.*, **16**(5), 601-609.

https://doi.org/10.12989/eas.2019.16.5.601.

Rabia, B., Daouadji, T.H. and Abderezak, R. (2019), "Effect of porosity in interfacial stress analysis of perfect FGM beams reinforced with a porous functionally graded materials plate", *Struct. Eng. Mech.*, **72**(3), 293-304. http://dx.doi.org/10.12989/sem.2019.72.3.293.

Reddy, J.N. and Cheng, Z.Q. (2001), "Three-dimensional thermomechanical deformations of functionally graded rectangular plates", *Eur. J. Mech.-A/Solid.*, **20**(5), 841-855. https://doi.org/10.1016/S0997-7538(01)01174-3.

Rezaei, A.S., Saidi, A.R., Abrishamdari, M. and Mohammadi, M.P. (2017), "Natural frequencies of functionally graded plates with porosities via a simple four variable plate theory: an analytical approach", *Thin Wall. Struct.*, **120**, 366-377. https://doi.org/10.1016/j.tws.2017.08.003.

Taibi, F.Z., Benyoucef, S., Tounsi, A., Bachir Bouiadjra, R., Adda Bedia, E.A. and Mahmoud, S.R. (2015), "A simple shear deformation theory for thermo-mechanical behaviour of functionally graded sandwich plates on elastic foundations", *J. Sandw. Struct. Mater.*, **17**(2), 99-129. https://doi.org/10.1177/1099636214554904.

Thai, H.T., Nguyen, T.K., Vo, T.P. and Lee, J. (2014), "Analysis of functionally graded sandwich plates using a new first-order shear deformation theory", *Eur. J. Mech.-A/Solid.*, **45**, 211-225. https://doi.org/10.1016/j.euromechsol.2013.12.008.

Tlidji, Y., Daouadji, T.H., Hadji, L., Tounsi, A. and Bedia, E.A.A. (2014), "Elasticity solution for bending response of functionally graded sandwich plates under thermomechanical loading", *J. Therm. Stress.*, **37**(7), 852-869. https://doi.org/10.1080/01495739.2014.912917.

Van Do, T., Nguyen, D.K., Duc, N.D., Doan, D.H. and Bui, T.Q. (2017), "Analysis of bi-directional functionally graded plates by FEM and a new third-order shear deformation plate theory", *Thin Wall. Struct*., **119**, 687-699. https://doi.org/10.1016/j.tws.2017.07.022.

Vu, T.V., Khosravifard, A., Hematiyan, M.R. and Bui, T.Q. (2018), "A new refined simple TSDT-based effective meshfree method for analysis of through-thickness FG plates", *Appl. Math. Model.*, **57**, 514-534. https://doi.org/10.1016/J.APM.2018.01.004.

Wang, Y., Ye, C. and Zu, J.W. (2018), "Identifying the temperature effect on the vibrations of functionally graded cylindrical shells with porosities", *Appl. Math. Model.*, **39**(11), 1587-1604. https://doi.org/10.1007/s10483-018-2388-6.

Winkler, E. (1867), "Die lehre von der elasticitaet und festigkeit", Prag Domin-icus, Prague.

Yaghoobi, H., Valipour, M.S., Fereidoon, A. and Khoshnevisrad, P. (2014), "Analytical study on post-buckling and nonlinear free vibration analysis of FG beams resting on nonlinear elastic foundation under thermo-mechanical loadings using VIM", *Steel Compos. Struct.*, **17**(5), 753-776. https://doi.org/10.12989/scs.2014.17.5.753.

Yin, S., Yu, T., Bui, T. Q., Zheng, X. and Tanaka, S. (2016), "In-plane material inhomogeneity of functionally graded plates: A higher-order shear deformation plate isogeometric analysis", *Compos. Part B: Eng.*, **106**, 273-284. https://doi.org/10.1016/j.compositesb.2016.09.008.

Yin, S., Yu, T., Bui, T.Q., Liu, P. and Hirose, S. (2016), "Buckling and vibration extended isogeometric analysis of imperfect graded Reissner-Mindlin plates with internal defects using NURBS and level sets", *Comput. Struct.*, **177**, 23-38. https://doi.org/10.1016/j.compstruc.2016.08.005.

Yu, T., Yin, S., Bui, T.Q., Liu, C. and Wattanasakulpong, N. (2017), "Buckling isogeometric analysis of functionally graded plates under combined thermal and mechanical loads", *Compos. Struct.*, **162**, 54-69. https://doi.org/10.1016/j.compstruct.2016.11.084.

Zenkour, A.M. (2010), "Hygro-thermo-mechanical effects on FGM plates resting on elastic foundations", *Compos. Struct.*, **93**, 234-238. https://doi.org/10.1016/j.compstruct.2010.04.017.

Zhu, J., Lai, Z., Yin, Z., Jeon, J. and Lee, S. (2001), "Fabrication of ZrO_2–NiCr functionally graded material by powder metallurgy", *Mater. Chem. Phys*., **68**(1-3), 130-135. https://doi.org/10.1016/S0254-0584(00)00355-2.